Tidal asymmetry and variability of bed shear stress and sediment bed flux at a site in San Francisco Bay, USA

Matthew L. Brennan[a], David H. Schoellhamer[b], Jon R. Burau[b] and Stephen G. Monismith[a]

[a]Environmental Fluid Mechanics Laboratory, Dept. Civil & Environmental Engineering, Stanford University, Stanford, CA, 94305-4020 USA.

[b]U. S. Geological Survey, Placer Hall, 6000 J St., Sacramento, CA 95819 USA

The relationship between sediment bed flux and bed shear stress during a pair of field experiments in a partially stratified estuary is examined in this paper. Time series of flow velocity, vertical density profiles, and suspended sediment concentration were measured continuously throughout the water column and intensely within 1 meter of the bed. These time series were analyzed to determine bed shear stress, vertical turbulent sediment flux, and mass of sediment suspended in the water column. Resuspension, as inferred from near-bed measurements of vertical turbulent sediment flux, was flood dominant, in accordance with the flood-dominant bed shear stress. Bathymetry-induced residual flow, gravitational circulation, and ebb tide salinity stratification contributed to the flood dominance. In addition to this flow-induced asymmetry, the erodibility of the sediment appears to increase during the first 2 hours of flood tide. Tidal asymmetry in bed shear stress and erodibility help explain an estuarine turbidity maximum that is present during flood tide but absent during ebb tide. Because horizontal advection was insignificant during most of the observation periods, the change in bed mass can be estimated from changes in the total suspended sediment mass. The square wave shape of the bed mass time series indicates that suspended sediment rapidly deposited in an unconsolidated or concentrated benthic suspension layer at slack tides and instantly resuspended when the shear stress became sufficiently large during a subsequent tide. The variability of bed mass associated with the spring/neap cycle (about 60 mg/cm^2) is similar to that associated with the semidiurnal tidal cycle.

KEY WORDS
estuaries, San Francisco Bay, suspended sediment, bed shear stress, stratification

1. INTRODUCTION

The flux of sediment between the bed and the water column, in response to variations in bed shear stress that occur in a partially stratified estuary, is examined in this paper. The net bed flux changes from erosion to deposition at tidal time scales, thereby controlling the amount of suspended sediment available for transport by the flow. When flow direction alternates with the tides, the tidally averaged (net) transport determines the ultimate fate of sediments. This net transport is created by asymmetry of flow and sediment response between flood and ebb tide. For example, Dronkers (1986) hypothesized that the peak

suspended sediment concentration at the landward limit of salt intrusion in an estuary may be created by an asymmetry in bed shear stress that creates landward flow to counteract the seaward river discharge.

Erosion from the bed to the water column is initiated by the shear stress exerted on the bed by the flow. As sinusoidal tidal currents accelerate, sediment is resuspended from the bed. Subsequently, the flow decelerates to the point that the net bed flux becomes dominated by deposition. However, the timing and magnitude of bed shear stress differs with each tidal phase, leading to a corresponding variability in bed flux. In the field, measurements of the Reynolds stress in the near-bed region provide a reasonable estimate of bed shear stress (Trowbridge et al., 1999).

The sources of variability that are examined in this paper are flood and ebb tides, spring and neap tides, and salt stratification and destratification. When flood and ebb react differently to channel bathymetry, a residual flow is created (Fischer et al., 1979). Spring-neap variations in barotropic forcing are caused by phasing differences between solar and lunar tidal components.

Vertical density gradients contribute to the bed shear stress asymmetry in a complex interaction with the barotropic forcing. The horizontal density gradient produces gravitational circulation that is directed landward at the bed and seaward at the surface, thereby strengthening bed shear stress on flood tide and weakening it on ebb tides. In addition to horizontal density gradients, vertical density gradients intermittently damp turbulent eddies, thereby reducing bed shear stress. Ebb tides tend to create stratification because vertical velocity shear advects fresher surface water over denser, saltier water, a process termed "strain induced periodic stratification" (SIPS) by Simpson et al. (1990). However, tidal flow also generates mixing, which breaks down stratification. Therefore, stratification is most prevalent during slack tides or less energetic neap tides (Stacey et al., 1999).

The balance between turbulence generation by fluid shear and turbulence suppression by density stratification is given by the gradient Richardson number, R_i

$$R_i = -(g \quad / \quad z) / (\ _0 (\ u/\ z)^2)$$

where g=gravitational constant, =fluid density as a function of only salinity, $_0$=mean fluid density, and z is the coordinate directed positive upwards from the bed. Turbulence tends to mix the water column when R_i is near zero. When R_i>0.25, turbulence is suppressed by density stratification (Itsweire et al., 1993), greatly diminishing mixing and allowing suspended particles to settle.

The relationship between bed flux and bed shear stress during a pair of field experiments conducted at a site in San Francisco Bay, California, is examined in this paper. Flow velocity, vertical density profiles, and suspended sediment concentration (SSC) were measured continuously throughout the water column over a 24-hour period in July 1997 and over a 9-day period in October 1999. These time series were analyzed to determine bed shear stress, vertical turbulent sediment flux, and mass of sediment suspended in the water column.

2. METHOD

2.1 Site bathymetry, hydrodynamics, and sediment characteristics

All the field data presented in this paper were collected in Suisun Cutoff, a tidal channel in northern San Francisco Bay, California (Figure 1). This channel is 2 km long and 500 m wide and has a nearly rectangular cross-section. While most of the channel is 10 m deep, a sill 2 m deep bounds the channel to the west and the east end deepens to 20 m. Approximately 65 km of water separates the site from the ocean.

A preliminary study was conducted on July 29-30, 1997, when the river discharge was approximately 300 m^3/s and spring tides prevailed. The second, more extensive, study from October 15-27, 1999, occurred just 1 month before the winter storm season, so river discharge at 100 m^3/s was near the year's minimum. In contrast, the annual peak flow averages approximately 3,000 m^3/s, and typically occurs between January and March. This second study began during a neap tide with a tidal range of 1.2 m and continued to a spring tide with a range of 1.5 m. Both experiments were situated in the center of Suisun Cutoff (approximately the top vertex of the triangle in Figure 1).

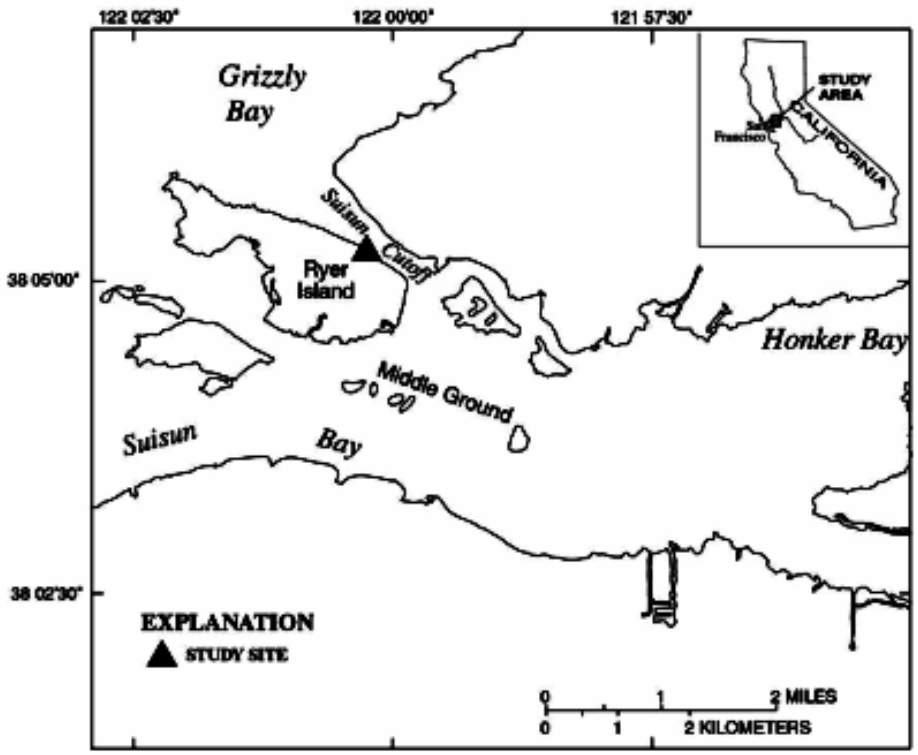

Figure 1. Study area - northern San Francisco Bay, California.

During the 1997 experiment, the balance created between the river discharge and the intruding salt resulted in salinity values of 4 to 9 on the practical salinity scale. With less river discharge during the 1999 study, the salinity increased, spanning a range from 8 to 16. Vertical gradients in salinity varied between well-mixed and stratified conditions, as is typical of a partially stratified estuary. Because maximum SSC observed during this study was approximately 200 mg/l and the vertical salinity gradient varied from 0 to 1 m^{-1}, salinity and temperature were the only constituents assumed to affect water density.

Although this work did not include sediment analysis, work by other researchers at nearby sites provides an estimate of sediment characteristics in Suisun Cutoff. Disaggregated size class analysis by Kineke and Sternberg (1989) indicates that suspended sediment is approximately 40% clay, 55% silt, and 5% sand, while bed sediment is 32% clay, 52% silt, and 16% sand. Sediment settling velocity has been estimated to be 10^{-3}-10^{-2} m/s (Sternberg et al, 1986, Kranck and Milligan, 1992). Kranck and Milligan (1992) also hypothesize that all but the largest flocs (>370 m) are "relatively stable particles which settled and were resuspended without much floc breakup."

2.2 Instrumentation

In 1997, we collected vertical profiles of velocity, density, and SSC at an anchor station for nearly 24 hours. A boat-mounted acoustic Doppler current profiler (ADCP) returned velocity vectors from every 0.25 m of the water column at a frequency of approximately 1 Hz. Concurrently, we sampled the vertical structure of salinity and SSC from the water surface to 0.25 m above the bed every 10 minutes with a manually operated instrument package. This instrument package contained probes for conductivity and temperature to estimate salinity, an optical backscatter sensor (OBS) to estimate SSC, as well as a pressure transducer to measure depth.

The 1999 experiment's instrumentation consisted of a pair of bed-mounted instrument frames and an autonomous water column profiler. These three instrument packages were located within 75 m of each other. One instrument frame carried an acoustic Doppler velocimeter (ADV) and an OBS that sampled the same measurement volume at 0.97 m above the bed. The ADV measured the three components of velocity (u, v, w) and acoustic backscatter intensity at 25 Hz. The OBS collected data at approximately 6 Hz. The frame also carried a conductivity sensor and a temperature sensor for determining salinity. The second frame carried an ADCP mounted 0.4 m above the bed. This instrument sampled velocity vectors in 25-cm intervals from 1.25 m above the bed to just below the water surface, collecting a complete profile at approximately 2 Hz. Communication cables connected these instruments to computers on board a boat anchored at the site.

The autonomous profiler consisted of a mechanical winch assembly mounted on the moored boat that lowered and raised an instrument package through the water column every 15 minutes. The instrument package measured vertical profiles of salinity and SSC, as in the 1997 experiment. However, the autonomous profiler used in 1999 only traversed water column from 1 m to 7 m below the surface, leaving the bottom 3 m unsampled. The 1997 data set provides the most complete picture of the near-bed region.

2.3 Data processing

All of the flow and sediment statistics were averaged into 10-minute blocks. This time interval reflects a balance between reducing uncertainty by increasing the number of samples and maintaining stationarity (Gross and Nowell, 1983). Whereas the ADCP has an internal compass and tilt sensor to establish its reference frame, the ADV data were rotated such that the mean vertical and cross-stream velocities in each 10-minute block were zero. In instances when the data from the autonomous profiler and ADCP were used simultaneously, the velocity was interpolated to coincide with the 15-minute interval of the autonomous profiler.

Backscatter intensity was converted to SSC through comparison with SSC estimates from gravimetric analysis of water samples collected in situ. For an OBS, the linear relationship between SSC and output voltage was determined using a repeated median fit (Buchanan and Ruhl, 2000) to decrease the influence of outliers on the regression. For the ADV, the intensity of returned acoustic energy is proportional to the logarithm of SSC (Thorne et al., 1993; Kawanisi and Yokosi, 1997). Before comparing ADV backscatter to water samples, the raw ADV backscatter data were treated to remove outliers. First, when measurements collected simultaneously from each of the ADV's three receivers differed by more than 5% of the mean intensity, the disparate values were discarded. Then, after averaging the three measurements, points further than five standard deviations from the 10-minute mean also were discarded. Between these two filters, no more than 2% of the data was eliminated.

The ADV estimates (SSC_{ADV}) of mean SSC are compared to the OBS estimates (SSC_{OBS}) in Figure 2. SSC_{ADV} only diverges significantly from SSC_{OBS} for approximately 1% of the data pairs. Values of SSC_{ADV} tend to be less than SSC_{OBS} at lower SSC values and greater than SSC_{OBS} at higher SSC values. The variance between the two measurements is a function of SSC, as expected from laboratory tests that indicate the direct relationship between OBS variance and SSC (Downing and Beach, 1989). When the absolute value of the difference between the two estimates is normalized by SSC_{OBS}, the mean percent error is 16%, which is comparable to the agreement of 10% between optical and acoustic backscatter sensors for sand, reported by Osborne et al. (1994).

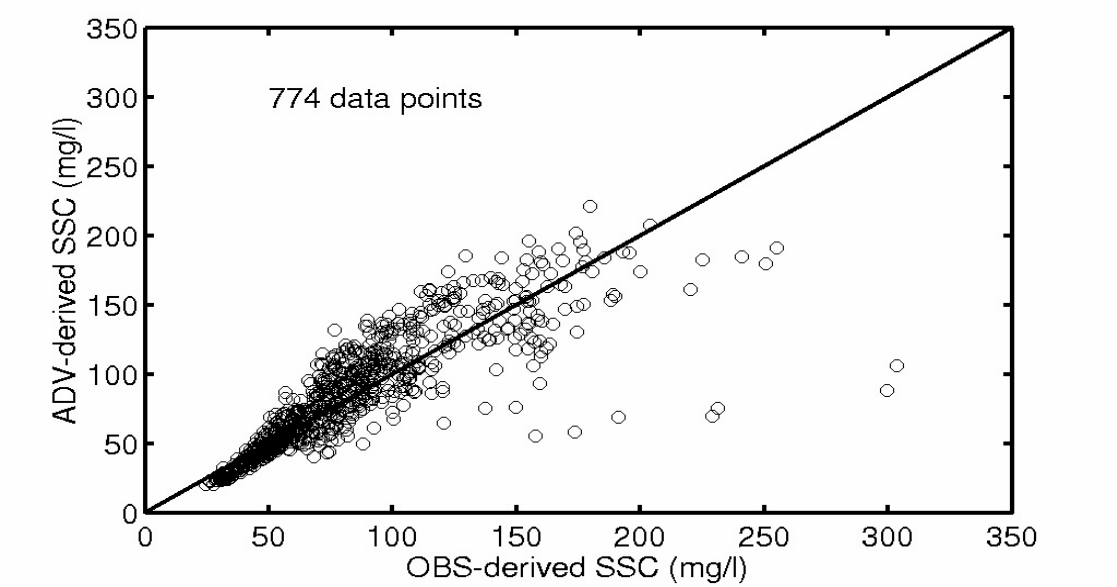

Figure 2. Comparison of ADV-derived SSC and OBS-derived SSC.

Concentration measurements derived from the ADV backscatter intensity were combined with the coincident velocity measurements from the ADV to estimate the turbulent vertical sediment flux, <w'c'>, where < > indicate a time average and primes indicate fluctuations from the mean.

Suspended mass was calculated from the vertical SSC profiles. For the 1997 data, suspended mass was calculated by summing SSC and multiplying by the uniform vertical

SSC sampling interval of 0.25 m, and the lowest sample point was 0.25 m above the bed. The 1999 data had nonuniform vertical spacing, suspended mass was calculated with the trapezoidal rule, and the lowest sample point was 0.97 m above the bed. Suspended mass will be underestimated because SSC measurements did not extend down to the bed, especially for the 1999 data.

Vertical profiles of density gradient were calculated from the CTD casts and vertical profiles of velocity gradient were calculated from the ADCP velocity profile data. The density and velocity gradient profiles then were used to calculate vertical profiles of the gradient Richardson number (R_i), which vary with time.

3. TIDAL ASYMMETRY OF BED SHEAR STRESS AND ERODIBILITY

3.1 Neap tide

The bed shear stress opposes the mean streamwise currents. These mean currents (U) measured at 0.97 m above the bed during the 1999 experiment, were flood dominated, as indicated in Figure 3A. This flood dominance runs counter to the estuary's overall seaward discharge of river water. This flood asymmetry probably results from residual flow created by the region's complex bathymetry (Stacey, 1996) and gravitational circulation, which contributes to landward flow in the near-bed region (Hansen and Rattray, 1966).

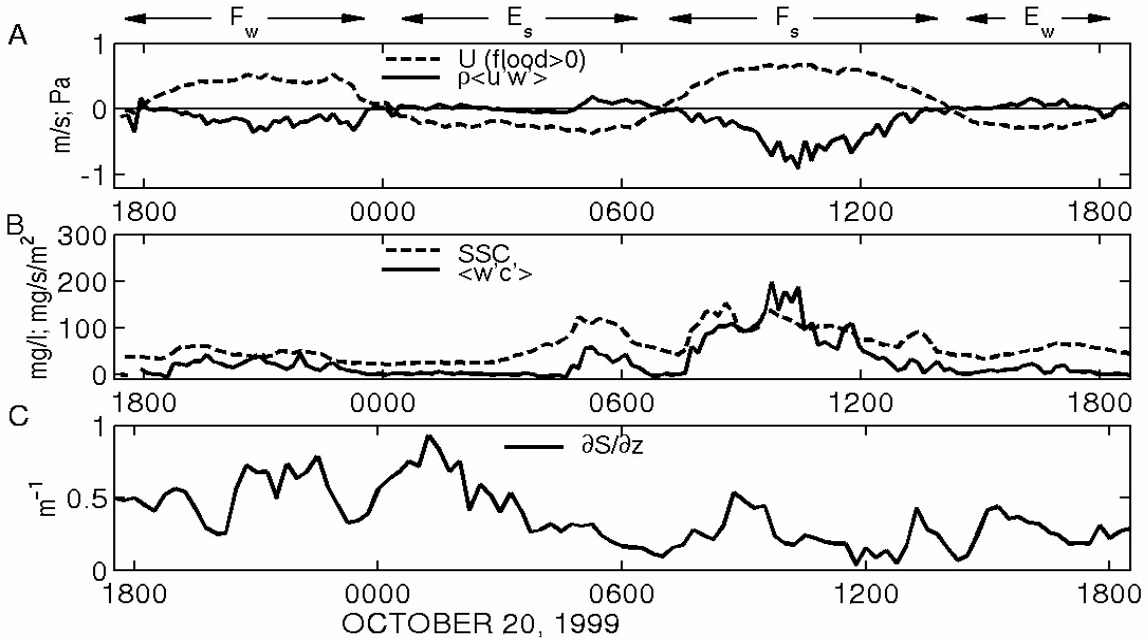

Figure 3. Measurements from October 1999 at 0.97 m above the bed: A) Time series of mean velocity (U) and Reynolds stress (<u'w'>) during neap tides. B) Time series of mean suspended sediment concentration (SSC), turbulent sediment flux (<w'c'>). C) Top-bottom vertical salinity gradient (S/ z).

As expected in light of the mean currents, the bed shear stress, as measured by the Reynolds stress, <u'w'>, also favored flood tides. In fact, the diurnal inequality created a cycle of four tides with different bed shear stress characteristics. The stronger flood (F_s) attained peak bed shear stress of 0.9 Pa and the weaker flood (F_w) attained a peak just over

0.4 Pa (Figure 3A). In contrast, the bed shear stress during the stronger ebb (E_s) and weaker ebb (E_w) reached a peak of just 0.1 Pa. As indicated in Figure 3C, strong salinity stratification existed between 1800 hours and 0430 hours. This period of strong stratification reduced bed shear stress during both the weaker flood and stronger ebb. This salinity stratification was particularly strong on the ebb tide, from 0000 to 0430 hours, when bed shear stress vanished even though the mean velocity reached speeds of 30 cm/s. This complete suppression of turbulence and bed shear stress were precipitated by SIPS, the ebb tide advection of fresh water on top of saltier water (Stacey et al., 2000).

ADV-derived time series of the turbulent sediment flux, <w'c'>, and the mean SSC are shown in Figure 3B. Over the course of a neap tidal day, the strong flood dominated the bed flux asymmetry. Turbulent sediment fluxes during the strong flood exceeded 150 mg/s/m^2, a magnitude at least three times the peak flux during the other tidal phases.

In the period 1800 to 0430 hours depicted in Figure 3B, changes in SSC correlated more strongly with <u'w'> and <w'c'> than the mean flow, because the flow was stratified. The turbulent sediment flux, <w'c'>, was considerably less during the weaker flood (1800-0000 hours) than <w'c'> during unstratified spring tides of only slightly larger magnitude (e.g. Figure 4B, 0000-0600 hours). At the beginning of the strong ebb in Figure 3B (0000-0430 hours), the mean flow accelerated to a magnitude that readily induced erosion during other tidal periods, but <w'c'> vanished, indicating that erosion may have been eliminated completely. After 0430 hours, when stratification had diminished, <w'c'> and SSC both increased rapidly.

Even though <u'w'> and <w'c'> are smaller and last for a shorter duration during the strong ebb, as compared to the weak flood, the peak SSC attained at the end of the strong ebb (0530 hours) is 30-50 mg/l larger than the peak attained during the weak flood. This suggests that horizontal advection contributed to SSC during the ebb. The rising edge of SSC that occurred during 0300-0430 hours, before the sharp increase in <u'w'> and <w'c'>, is another signal of advection-induced SSC.

3.2 Spring tide

The more energetic spring tides later in the experiment produced larger bed shear stresses in all phases of the tidal day (Figure 4A). The flood still dominated, with the peak bed shear stresses of 1.1 Pa and 0.8 Pa during the stronger and weaker floods, respectively. Bed shear stress on the stronger ebb was comparable to that of the weaker flood, while the weaker ebb yielded peaks of only 0.2 Pa. Turbulent mixing was greater than during neap tide, such that periods of vertical stratification were weaker and lasted only 1-2 hours around slack tides (Figure 4C), minimizing stratification's influence on sediment bed flux.

In contrast to only one large resuspension event during a neap tidal day (Figure 3B), significant resuspension events occurred on three of four tides comprising the spring tidal day (Figure 4B). The turbulent sediment flux peaked at 120-180 mg/s/m^2 during the weaker flood, the stronger flood, and the stronger ebb, as compared to the peak of only 20 mg/s/m^2 during the weaker ebb. Hence, the relative absence of resuspension during the weaker ebb leads to a net flood asymmetry in bed flux.

Around the time of peak flow velocity, decreasing SSC coincided more closely with the decline in the turbulent quantities, <u'w'> and <w'c'>, than the deceleration of the mean flow. For example, SSC, <w'c'>, and <u'w'> began to decline at 1400 hours on October 25, but the mean velocity stayed nearly constant for another hour (Figure 4B). This behavior

parallels oobservations by Sanford and Halka (1993). These authors propose that this response may be modeled best by continuous deposition, rather than the widely-used model (Krone, 1962), in which deposition occurs only when the bed shear stress falls below a certain value. Sanford and Halka (1993) suggest two possible explanations for the disjoint between these deposition models; differences between laboratory and field flow scaling or the effect of a distribution of sediment sizes.

While <w'c'> was proportional to bed shear, the relation was not temporally uniform. Turbulent sediment flux was most responsive to <u'w'> at the beginning of flood tides, as indicated by the steeper slope of data points from the first 2 hours of flood (Figure 5). The slope's steepness was less during all other times of the tidal cycle, which may indicate the sediment's degree of erodibility.

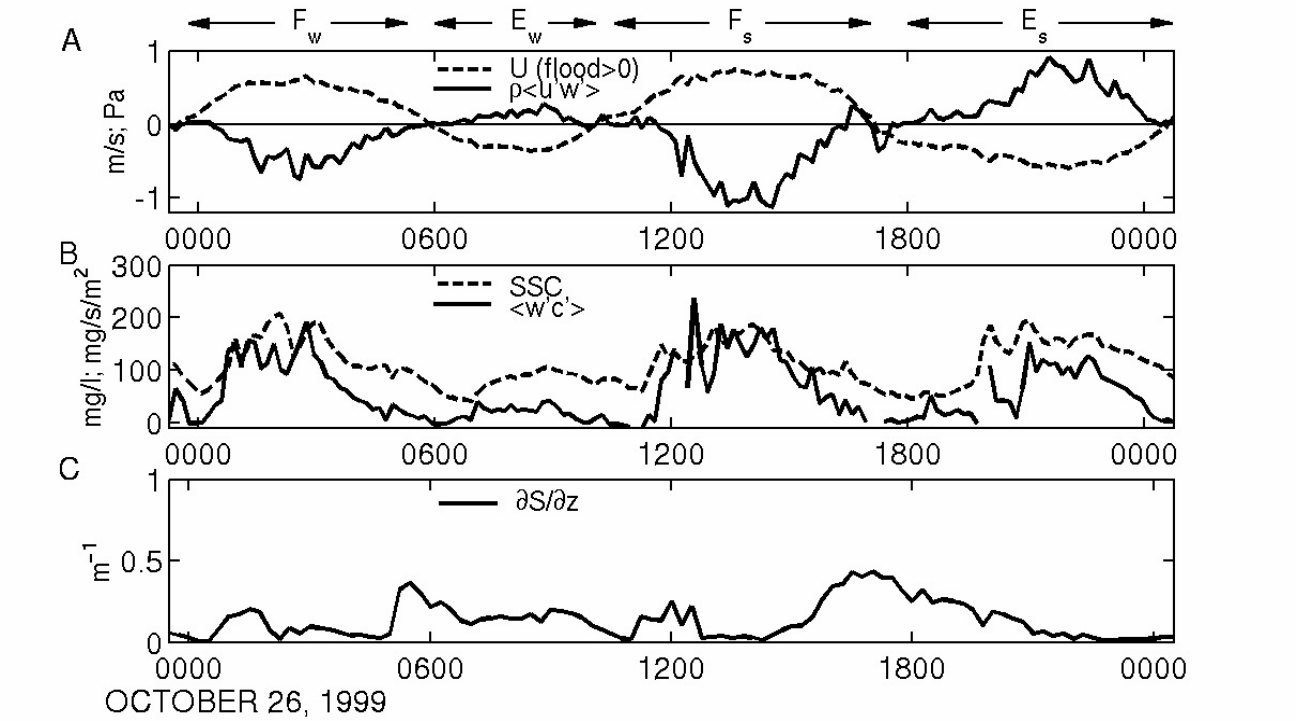

Figure 4. Measurements from October 1999 at 0.97 m above the bed: A) Time series of mean velocity (U) and Reynolds stress (r<u'w'>) during spring tides. B) Time series of mean suspended sediment concentration (SSC), turbulent sediment flux (<w'c'>). C) Top-bottom vertical salinity gradient (S/ z).

Salinity enhancement of bottom sediment shear strength or bioturbation may explain this asymmetry in erodibility. Sediment deposited at the end-of-ebb salinity of 8 had less shear strength than sediment deposited at the greater end-of-flood salinity of 14. Sediment shear strength has increased to salinities of 10 in laboratory experiments (Parchure and Mehta, 1985). Or perhaps clams (*Potamocorbula amurensis*), which inhabit the bed in Suisun Cutoff at densities of several thousand per square meter, are a source of bioturbation during the beginning of flood tides (J. Thompson, U.S. Geological Survey, oral communication, 2000). They typically feed on the bed surface during ebb tides, which carry a larger nutrient load from river discharge. When the tide switches to flood, the clams actively bury themselves

into the mud. Finally, the asymmetry may not be related to the sediment erodibility at all; it may be caused by horizontal advection. Because the magnitude of concentration fluctuations scale with the mean SSC, the increase in <w'c'> at the start of flood may result from advection of a more turbid water mass into the ADV control volume. Most of the time, however, SSC increases correspond to increased bed shear stress, so advection does not seem to be a likely explanation.

Whatever the mechanism, the asymmetry in erodibility combined with the asymmetry of bed shear to create a mean landward flux of sediment of 14 g/s/m^2 over the 8 days of ADV data from this experiment.

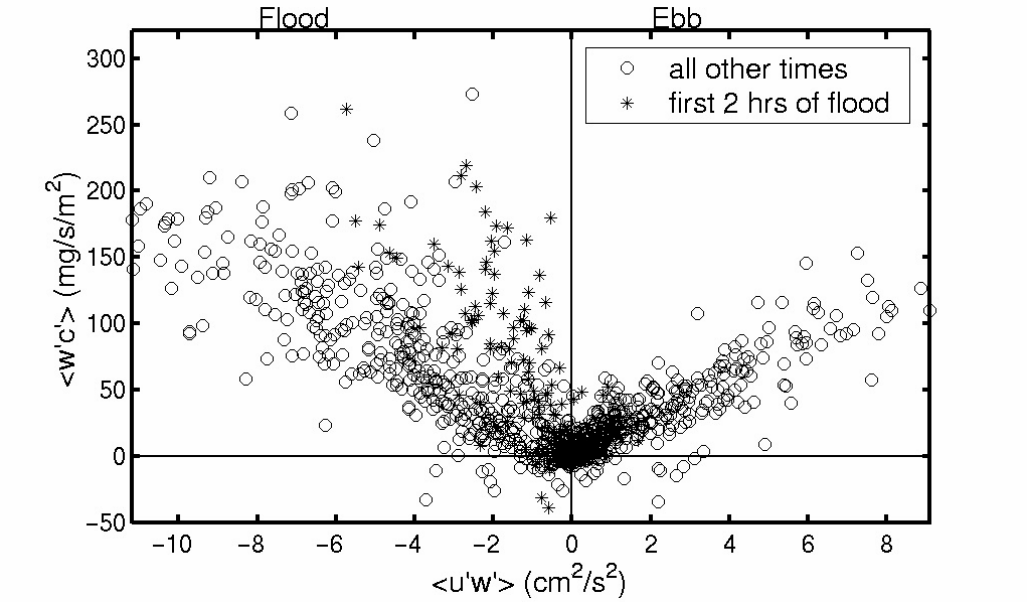

Figure 5. Turbulent sediment flux (<w'c'>) response to Reynolds stress (<u'w'>) during the first two hours of flood (negative <u'w'>) and all other times during the October 1999 experiment. Measurement volume is 0.97 m above the bed.

3.3 Effect on the estuarine turbidity maximum

Tidal asymmetry of bed shear stress and erodibility help explain an estuarine turbidity maximum in Suisun Bay at salinities of 1 to 6 during flood tides that is absent during ebb tides (Schoellhamer, 2001). During neap tides, tidal asymmetry of bed shear stress is most pronounced, and during (neap) flood tides, an estuarine turbidity maximum is regularly observed in the eastern side of Suisun Bay at salinities less than 5.

4. TIDAL VARIABILITY IN SUSPENDED AND BED MASS

Variability of SSC on the tidal time scale during the 1997 experiment was controlled by density stratification of the water column, vertical mixing, resuspension, and deposition. SSC varied inversely with the gradient Richardson number, R_i. As R_i decreased, turbulence and vertical mixing increased, which increased SSC. In 1997, SSC decreased during a slack after flood tide at 1500 hours on July 29 as turbulence in the water column diminished (Figure 6B). A weak ebb tide followed until 1800 hours that failed to disrupt stratification

and resuspend the deposited bottom sediment. At 2000 hours, a flood tide mixed the water column and increased SSC. Turbulence vanished during a slack tide at 0000 hours on July 30 and SSC decreased as suspended sediment deposited. A stronger ebb tide mixed the water column and resuspended bottom sediment at 0300 hours.

Changes in SSC were controlled by local stratification, turbulent mixing, and settling — not horizontal advection. At slack tides, turbulence vanished and suspended sediment deposited on the bed. The time scale of settling (depth divided by settling velocity) is on the order of 1 hour, which is about the duration of suppressed turbulence at slack tide. If the subsequent tide was strong enough to break down stratification, then bottom sediment resuspended into the water column. The 1997 data were collected during a spring tide when increased tidal energy mixed the water column during most tides. Horizontal advection of suspended sediment did not appear to be significant, as indicated by rapid decreases in SSC at slack tide, when advection would be small and rapid increases in SSC were concurrent with generation of turbulence in the water column.

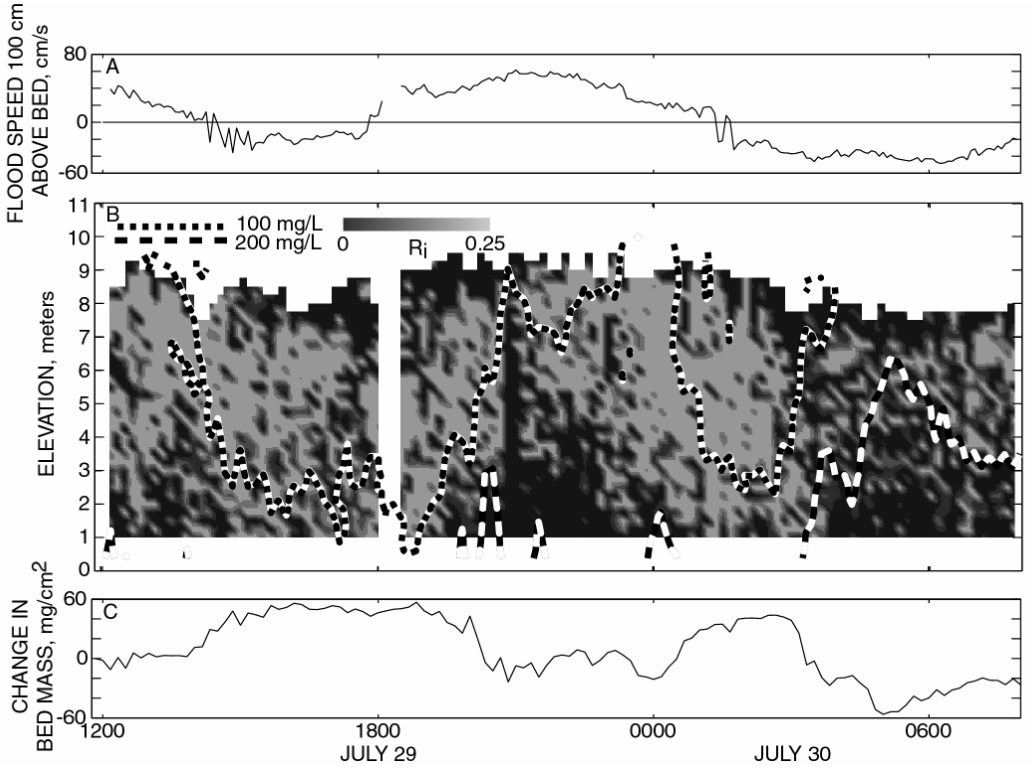

Figure 6. A) Flood current speed 100 cm above the bed. B) Vertical profiles of Richardson number and contours of suspended-sediment concentration. C) Change in mass of sediment on the bed, Suisun Cutoff, July 1997.

Because local deposition and resuspension controlled SSC, the change in bed mass can be assumed to be opposite of the change in suspended mass. Mass of suspended sediment was calculated by integrating the vertical profiles of SSC as described previously.

The time series of bed mass appears similar to a square wave (Figure 6C) due to bed flux. A greater quantity of sediment was on the bed near slack tides and during the weak ebb tide on July 29. When the velocity was great enough to resuspend sediment, about 60

mg/cm^2 were resuspended almost instantly. After this initial resuspension (sometimes called bulk erosion), there was no significant change in bed mass until the following slack tide because the remaining bottom sediment had sufficient shear strength to resist (mass) erosion. When the current and turbulence decreased, the same quantity of sediment (60 mg/cm^2) rapidly deposited. Assuming that the dry density of the deposit was on the order of 100 mg/cm^3, the depth of the deposit was on the order of several millimeters. After this initial deposition, the bed mass remained roughly constant because turbulence in the water column was able to keep the remaining suspended sediment in suspension. Thus, about 60 mg/cm^2 appeared to rapidly deposit in an unconsolidated layer with little shear strength. This layer was instantly resuspended when the shear stress became sufficiently large. Otherwise, the rates of erosion and deposition were relatively small.

The observed weak transient deposit may be better defined as a concentrated benthic suspension (CBS), which Winterwerp (2002) predicted will form for similar water depth (8 m), tidal velocity (50 cm/s), and settling velocity (0.5 mm/s), but greater mean SSC (290 mg/L), and no salinity stratification. Mean SSC at our study site was smaller, which would lessen the chance that a CBS would form. Turbulence damping by salinity stratification at our study site, however, may increase the chance that a CBS would form. Mehta (1989) presented idealized vertical profiles of SSC that included fluid mud, similar to CBS, at the interface of the water column and cohesive bed.

5. SPRING/NEAP VARIABILITY OF SUSPENDED AND BED MASS

Suspended and bed mass also vary with the spring/neap cycle. The October 1999 instrument deployment began during a neap tide and finished during a spring tide 9 days later. Stratification and turbulent mixing are described in detail by Stacey et al. (2000).

During the neap tides from October 16-20 the water column usually was stratified, turbulence usually was suppressed, and SSC and bed flux were small (Figure 7B). Salinity-induced periodic stratification (SIPS) was created during ebb tides and vanished during strong flood tides, which was when turbulence was generated and SSC and suspended mass increased. SSC and suspended mass also increased during ebb tides, though there was little turbulence; this was probably due to advection of more turbid water from shoals at Middle Ground and the shallow subembayment, Honker Bay. During neap tides, resuspension was smaller and, therefore, did not mask advection, unlike spring tides. Measurements of <w'c'> (Figure 3B) also help to differentiate increases in suspended mass due to resuspension and advection. The change in suspended mass during neap tides probably is equal to the change in bed mass during slack tide deposition and flood tide resuspension when local resuspension or deposition dominate horizontal advective transport. The change in bed mass during these phases of the tidal cycle ranges from about 0-20 mg/cm^2.

The more energetic spring tides around October 23-27 periodically generated turbulence, mixed the water column, resuspended bottom sediment, and increased SSC (Figure 7B). Most of the changes in suspended mass were associated with increased turbulence, resuspension, and mixing or turbulence suppression, slack tide, and deposition. As in 1997, suspended mass, and, thus, usually bed mass, varied similar to a square wave with a height of about 60 mg/cm^2 during spring tide (Figure 7C).

Assuming that changes in suspended mass generally are opposite to changes in bed mass, the tidal variability and total quantity of bed mass change from neap to spring tide. Tidal variability of bed mass increases from 0-20 mg/cm^2 during neap tide to about 60

mg/cm^2 during spring tide because the more energetic spring tides increase resuspension, SSC, and deposition flux. These quantities represent the size of the unconsolidated layer that deposits during slack tide and erodes easily during the subsequent tide. During slack tides, when suspended mass is smallest and bed mass is greatest, bed mass is about 20 mg/cm^2 less during spring tides than during neap tides. During maximum tides, when bed mass is smallest, bed mass is about 80 mg/cm^2 less during spring tides than during neap tides. Assuming that the dry density of the deposit was on the order of 100 mg/cm^3, the elevation of the bed varied by several millimeters between neap and spring tide. Therefore, bed flux associated with the spring/neap cycle is similar to that associated with the semidiurnal tidal cycle.

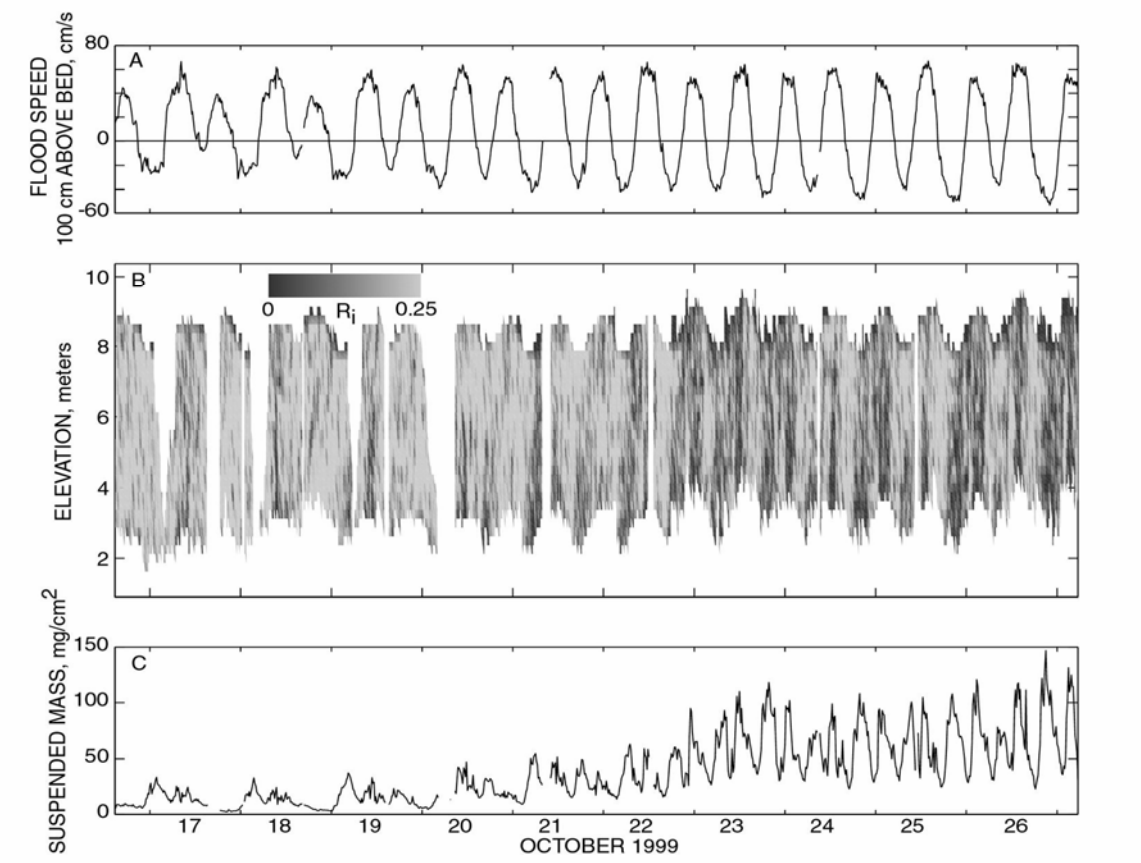

Figure 7. A) Flood current speed 100 cm above the bed. B) Vertical profiles of Richardson number. C) Mass of suspended sediment, Suisun Cutoff, October 1999.

The variations in total suspended mass agree qualitatively with the ADV suspended sediment measurements. For example, the suspended mass data (Figure 7C) and the ADV data (Figure 3B and Figure 4B) both show increases by a factor of two to three between neap tide and spring tide. Additionally, the second peak in suspended mass on October 26 (Figure 7C) is considerably less than the three other peaks on that day, which corresponds to the much lower <w'c'> shown in Figure 4B during the weaker ebb (0600-1000 hours). Finally, the <w'c'> time series concurs with the square wave behavior of the total suspended mass. For instance, the rapid increase in <w'c'> at the beginning of each of the stronger tides in

Figure 4B (0100, 1200, and 2100 hours), corresponds to the period of rapid resupension which generates the steep rises of the square wave in Figure 7C. Also, the constant peak in the suspended mass which appears as the square wave plateaus (e.g. Figure 6C, 1500-2000 hours) are matched by similar peak plateaus in <w'c'> (e.g. Figure 4B, 1200-1500 hours). These plateaus of constant suspended mass are produced by the equilibrium condition of constant, upwards <w'c'> balancing downwards settling flux (product of particle settling velocity and mean concentration). Quantitative comparison between the ADV data and the total suspended mass data are not viable, because the ADV's small sampling volume (~1 cm^3) does not capture significant vertical variations over the 7 meters of water column integrated to obtain total suspended mass.

6. CONCLUSIONS

The bed shear stress, as inferred from the Reynolds stress, <u'w'>, is flood-dominated at this study's field site. Tidal pumping around the site's complex bathymetry and gravitational circulation induced by horizontal density gradients contribute to the mean flow flood asymmetry. Stratification contributes to this asymmetry by preferentially suppressing turbulent mixing, particularly on ebbing neap tides.

These three factors produce a corresponding asymmetry in bed flux, as estimated from the vertical turbulent sediment flux, <w'c'>. During neap tides, bed flux was approximately three times larger during the stronger flood, as compared to the three other tidal periods of the tidal day. This flood dominance is created, in part, by periods of strong stratification on ebbing neap tides. The stratification completely suppresses turbulence and resuspension for two-thirds of the stronger ebbs, though mean velocity exceeds values that induce erosion during other phases of the tide. During spring tides, the net flood bed flux asymmetry is created, in large part, by the lack of resuspension during the weaker ebb. In addition, the flood asymmetry is augmented by changes in sediment erodibility. During the first two hours of flood tide, sediment erodibility apparently increases, as compared to other times in the tidal cycle. Tidal asymmetry in bed shear stress and erodibility help explain an estuarine turbidity maximum that is present during flood tide but absent during ebb tide.

During periods of decelerating flow (e.g. 1400 hours in Figure 4), SSC declines in concert with <u'w'> and <w'c'>, while mean velocity maintains its peak value for about another hour. This behavior replicates the sediment response reported by Sanford and Halka (1993). These authors modeled this SSC behavior with continuous deposition, as opposed to the standard model of bed-shear-stress dependent deposition.

During spring tides and some phases of neap tides, changes in SSC were controlled by local stratification, turbulent mixing, and settling--not horizontal advection. When local bed flux controlled SSC, the change in suspended mass can be assumed opposite of the change in bed mass. At slack tide, suspended sediment rapidly deposited in an unconsolidated layer with little shear strength. This layer, which may be a concentrated benthic suspension, was instantly resuspended when the shear stress became sufficiently large during a subsequent tide. Otherwise, the rates of erosion and deposition were relatively small. The resulting time series of bed mass appear similar to a square wave. This tidal variability of bed mass increased from 0-20 mg/cm^2 during neap tide to about 60 mg/cm^2 during spring tide because the more energetic spring tides increase resuspension. This would produce changes of several

millimeters in bed elevation. The variability of bed mass associated with the spring/neap cycle is similar to that associated with the semidiurnal tidal cycle.

ACKNOWLEDGMENTS

The authors thank Jon Yokomizo, Jim George, Jay Cuetara, Jessica Lacy, Cary Troy, Catherine Ruhl, Rob Sheipline, Mark Stacey, Jim DeRose, and Brad Sullivan for helping collect these data. Mark Stacey and Ray Krone reviewed previous versions of this paper. This study was supported by the U.S. Geological Survey Place-Based Program, the U.S. Office of Naval Research, the Interagency Ecological Program for the Sacramento-San Joaquin Estuary, and the Burt and Deedee McMurtry Stanford Graduate Fellowship.

REFERENCES

Buchanan, P.A. and Ruhl, C.A., 2000, Summary of suspended-solids concentration data, San Francisco Bay, CA, water year 1998, *U.S. Geological Survey Open File Report* 00-88, 41 p.

Downing, J.P. and Beach, R.A., 1989, Laboratory apparatus for calibrating optical suspended solids sensors, *Marine Geology*, (86) 243-249.

Dronkers, J., 1986, Tide-induced residual transport of fine sediment, *Physics of Shallow Estuaries and Bays*, ed. J. Van de Kreeke, Springer-Verlag, 228-244.

Fischer, H.B., List, E.J., Imberger, J. and Brooks, N.H., 1979, *Mixing in inland and coastal waters*, Academic Press Inc., 483 p.

Gross, T.F. and Nowell, A.R.M., 1983, Mean flow and turbulence scaling in a tidal boundary layer, *Continental Shelf Research*, (2) 2/3, 109-126.

Hansen, D.V. and Rattray, M., 1966, Gravitational circulation in straits and estuaries, *Journal of Marine Research*, (23) 2, 104-122.

Itsweire, E.C., Koseff, J.R., Briggs, D.A., and Ferziger, J.H., 1993, Turbulence in stratified shear flows: implications for interpreting shear-induced mixing in the ocean, *Journal of Physical Oceanography*, (23), 1508-1522.

Kawanisi, K. and Yokosi, S., 1997, Characteristics of suspended sediment and turbulence in a tidal boundary layer, *Continental Shelf Research,* (17) 8, 859-875.

Kineke, G.C. and Sternberg, R.W., 1989, The effect of particle settling velocity on computed suspended sediment concentration profiles, *Marine Geology*, (90) 3, 159-174.

Kranck, K. and Milligan, T.G., 1992, Characteristics of suspended particles at an 11-hour anchor station in San Francisco Bay, California, *Journal of Geophysical Research*, (97) C7, 11,373-11,382.

Krone, R. B., 1962, Flume studies of the transport of sediment in estuarial shoaling processes, *Final Report*, University of California, Berkeley, Hydraulic and Sanitary Engineering Research Lab. 110 p.

Mehta, A.J., 1989, On estuarine cohesive sediment suspension behavior, *Journal of Geophysical Research*, (94) C10, 14,303-14,314.

Osborne, P.D., Vincent, C.E. and Greenwood, B., 1994, Measurement of suspended sand concentrations in the nearshore: field intercomparison of optical and acoustic backscatter sensors, *Continental Shelf Research*, (14) 2-3, 159-174.

Parchure, T.M., and Mehta, A.J., 1985, Erosion of soft cohesive sediment deposits, *Journal of Hydraulic Engineering*, (111) 10, 1308-1326.

Sanford, L.P. And Halka, J.P., 1993, Assessing the paradigm of mutually exclusive erosion and deposition of mud, with examples from upper Chesapeake Bay, *Marine Geology*, (114) 1-2, 37-57.

Schoellhamer, D.H., 2001, Influence of salinity, bottom topography, and tides on locations of estuarine turbidity maxima in northern San Francisco Bay, *Coastal and Estuarine Fine Sediment Transport Processes*, ed. W.H. McAnally, and A.J. Mehta, 343-357.

Simpson, J.H., Brown, J., and Matthews, J. and Allen, G., 1990, Tidal straining, density currents, and stirring in the control of estuarine stratification, *Estuaries*, (13) 125-132.

Stacey, M.T., 1996, Turbulent mixing and residual circulation in a partially stratified estuary, Ph.D. Dissertation, Stanford University.

Stacey, M.T., Monismith, S.G., and Burau, J.R., 1999, Observations of turbulence in a partially stratified estuary, *Journal of Physical Oceanography*, (29) 1950-1970.

Stacey, M.T., Burau, J.R., Brennan, M.L., Lacy, J., Tobin, C. C., and Monismith, S.G., 2000, Spring-neap variations in stratification and turbulent mixing in a partially stratified estuary, Proceedings *5th International Symposium on Stratified Flows*, ed. G.A. Lawrence, R. Pieters, and N. Tomemitsu, 939-944.

Sternberg, R.W., Cacchione, D.A., Drake, D.W. and Kranck, K., 1986, Suspended sediment transport in an estuarine tidal channel within San Francisco Bay, California, *Marine Geology*, (71) 3-4, 237-258.

Thorne, P.D., Hardcastle, P.J., and Soulsby, R.L., 1993, Analysis of acoustic measurements of suspended sediments, *Journal of Geophysical Research*, (98) C1, 899-910.

Trowbridge, J.H., Geyer, W.R., Bown, M.M. and Williams, A.J., 1999, Near-bottom turbulence measurements in a partially mixed estuary: turbulent energy balance, velocity structure and along channel momentum balance, *Journal of Physical Oceanography*, (29) 12, 3056-3072.

Winterwerp, J.C., 2002, Scaling parameters for high concentration mud suspensions under tidal conditions. Proceedings *INTERCOH-2000, Elsevier, Coastal and Estuarine Fine Sediment Processes*, ed. J.C. Winterwerp and C. Kranenburg, this volume.